The atmospheric boundary layer in an Alpine valley during wintertime persistent temperature inversions

Gabriele Arduini[1,2], Charles Chemel[2], Chantal Staquet[1], Stella Todzo[1], Florence Troude[3]

[1] LEGI, University Grenoble Alpes/CNRS, France
[2] Center for Atmospheric and Instrumentation Research, University of Hertfordshire, UK
[3] Air Rhône-Alpes, 3 Allée des Sorbiers, 69500 Bron, France
Chantal.Staquet@legi.grenoble-inp.fr

Abstract

The atmospheric circulation during persistent wintertime temperature inversions in an Alpine valley is investigated within the context of the Passy valley, which is the strongest polluted place in the French Alps when such inversions occur. An idealized version of the topography of this valley is designed and introduced in the atmospheric numerical model WRF, consisting in a valley which narrows by a factor of 10 before opening on a plain. Numerical results show that an up-valley wind develops during the first part of the night, before reversing and becoming down-valley as usually observed for a nocturnal along-valley wind. The wind speed is very weak, of the order of $1\,\mathrm{m\,s^{-1}}$, implying that the ventilation in the valley toward the plain is first halted before resuming at a very low speed. Analysis of a field campaign held in January-February 2015 in the Passy valley is eventually briefly presented using Lidar data.

1 Introduction

In a valley at sunset, downslope winds form as a result of the radiative cooling of the ground: the air layer close to the ground cools and flows down by gravity (f.i. Whiteman, 2000). The downslope-advected cold air fills the bottom of the valley which, together with the radiative cooling at the valley bottom, results in a cold air pool. In winter, this cold air pool is often associated with a positive temperature gradient and is referred to as a temperature inversion. In the simplest case of a valley opening on a plain, the air at a given altitude is colder in the valley than over the plain leading to a pressure gradient which triggers a down-valley wind. Downslope and down-valley winds are the main elements of the valley-wind system. In winter, inversions usually extend from the bottom to the top of the valley and can last for a few days to several weeks, being triggered and maintained by an anticyclonic regime at synoptic scale. These inversions will be referred to as *persistent inversions* in the following[1]. Synoptic winds are usually very weak during an anticyclonic regime implying that the inversion layer is often weakly coupled to the free troposphere. The valley-wind system therefore controls the atmospheric circulation in the valley during a persistent inversion.

Studies of persistent inversions in complex terrain are generally motivated by fog formation at critical sites and by air quality concerns in urbanized areas. Urbanized sites are indeed very sensitive to temperature inversions. Pollutants emitted by traffic, industry and domestic heating are trapped in the inversion layer (Fig. 1a), thereby accumulating during a persistent inversion and inducing well-documented health impact.

[1]Persistent inversions should be distinguished from the diurnal inversions which form at night, even in summer, and are destroyed each morning by convective activity from the ground.

Several field campaigns dedicated to the study of wintertime persistent inversions in complex terrain have been conducted, with gradual focusing on smaller scales and growing importance of numerical studies for planning and conducting the field studies and analysing the data. Campaigns were mainly held in the United States, the atmospheric circulation in the Salt Lake valley having been extensively investigated recently (Lareau et al., 2013) along with the impact of persistent inversions on air quality (Silcox et al., 2012). As for the Alps, the first wintertime field campaign aiming at studying persistent inversions was held in the Arve valley in France in January and February 2015, motivated by the anomalously high pollution level frequently recorded around the city of Passy in this valley. Both meteorological and chemical data were collected during the campaign, referred to as the Passy-2015 campaign (Paci et al., 2015; Staquet et al., 2015; Chemel et al., 2016).

The purpose of the present paper is to get insight into the dynamical processes that may promote the high pollution level recorded around the city of Passy. More precisely, focus is made on the impact of the topography of the valley on these dynamical processes. An idealized configuration will be first considered in section 3, using numerical modeling, before data from the Passy-2015 field campaign are analyzed in section 4.

2 The Passy valley and the measurement site

A view of the Arve valley around Passy is displayed in Fig. 1b. This section of the valley, of moon shape, has two constrictions which are indicated on the figure: a narrowing of the valley downstream, with a width of 150 m, just after Marnaz, and a 250-m height sill upstream, before Chamonix located 15 km away eastward. The section of the Arve valley between these two constrictions will be referred to as the *Passy valley* hereafter. The Passy valley has two tributary valleys on its south side. The dimensions of the valley, indicated in the caption of Fig. 1b, show that the valley is both steep and narrow.

(a) (b)

Figure 1: Left frame: View of the Arve valley in Passy on the polluted day of February 11, 2015. Right frame: Satellite image of the Passy valley, defined as the part of the Arve valley comprised between the two constrictions (red symbols), and main measurement site of the field campaign (purple symbol). The distance between the two constrictions when following the valley is 25 km. The largest width of the Passy valley is 2 km, implying that the valley is very narrow. It is also very steep: the summit over Passy peaks at 2700 m while the altitude of the valley bottom is 560 m. Away from the sill, the valley slope between the two constrictions is very gentle, of 0.4%. Image from Google Earth.

3 A simple idealized model of the Passy valley

3.1 Design of the idealized model

A simple idealized representation of the Passy valley consists of a system of two valleys opening on a plain, ignoring the curvature and the tributaries. The summits on either

side of the valleys are replaced by plateaux with altitude 1800 m, the valley bottom being located at 1000 m. This simple topography was introduced in the numerical model WRF (Weather Research and Forecast, version 3.4.1), the valley axis coinciding with the $y-$axis. The WRF model solves the compressible Navier-Stokes equations over a complex terrain. Two nested domains were used, the valley system and part of the plain being introduced in the inner domain. To handle boundary conditions more easily, the topography was made even-symmetric at its upstream end with respect to a vertical $(x-z)$ plane. Therefore the along-valley wind vanishes at the upstream end, which partly mimicks the sill. Indeed, because a cold air pool develops from the valley bottom, the along-valley wind also vanishes at the sill bottom. The boundary conditions are applied to the outer domain and are of the open type in the $y-$ direction and of the periodic type in the $x-$ direction. A soil model is used and the surface forcing (which cools the air surface layer in the present case) is simulated by coupling the land surface model to the atmospheric model using the Monin-Obukov similarity theory. Simulations are started one hour before sunset during wintertime and are run over 6 hours. No velocity field is imposed at the initial time and the potential temperature profile is linear, of vertical gradient $1.5\,\mathrm{K\,km^{-1}}$. In the inner domain, the resolution is 90 m in the horizontal and of 2 m close to the ground along the vertical. More details are provided in Arduini et al. (2016a).

Two different configurations of the valley system will be considered, for which the upstream valley will be either larger or narrower than the downstream valley, these cases being referred to as draining (D1) and pooling (P1), respectively (Fig. 2). A so-called reference case (I1) will also be considered, in which the upstream valley opens directly to a plane. To mimick the dimensions of the Passy valley, a second pooling case will be run (P2), in which the ratio of the upstream and downstream valleys will be about 10. For numerical reason, the upstream valley width in this P2 case is different from that in P1 so that a second reference case was carried out (I2).

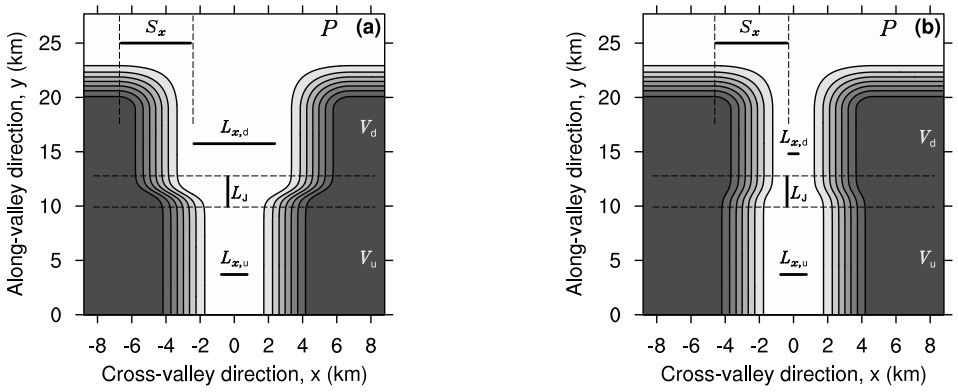

Figure 2: Sketch of the valley system for the draining case D1 (left) and the pooling case P1 (right). In I1, D1 and P1, the upstream valley width is equal to 720 m. In I2 and P2, this value is equal to 2070 m. As for the downstream valley width, it is equal to 2070 m for D1 and to 180 m for P1 and P2. I1 and I2 are reference cases in which the upstream valley opens directly to the plain. For all cases, the length of the upstream and downstream valleys is 10 km and 6 km, respectively, the junction length between the two valleys being 3 km.

3.2 The flow behavior in a valley opening to a plain

When a valley opens to a plain, the flow behavior from sunset can be decomposed into two stages, as analysed in Arduini et al. (2016b). Downslope flows on both slopes of the

valley advect cold air toward the valley bottom which, in addition to the cooling of the surface air layer by long wave radiation from the ground, creates a cold air pool. The convergence of the downslope winds at the valley center induces vertical motions by mass conservation which increases the height of the cold air pool. No such cold air pool exists of course over the plain as only radiative cooling of the surface is present. Consequently, a pressure gradient sets in between the valley and the plain thereby driving a down-valley wind. This down-valley wind first develops at the valley exit, close to the plain, before draining air further upstream in the valley. The down-valley wind suppresses the vertical motions and therefore the growth of the cold air pool. A steady state is eventually reached in the atmospheric boundary layer which, for the along-valley wind, is well described by the Bernoulli equation. The time scale for this steady state to be reached is proportional to $L_{tot}/(HN)$, where L_{tot} is the total valley length, H is the valley depth and N is the Brunt-Vaisala frequency outside the inversion layer, assumed to be constant (Egger, 1990). In the cases analyzed by Arduini et al. (2016b), which are qualitatively similar to the reference cases I1 and I2, the proportionality constant is found equal to 6, as in Schmidli and Rotunno (2015).

3.3 The flow behavior in a system of two valleys opening on a plain

The pooling cases P1 and P2 are first discussed before a brief account of case D1 is provided. In the following, the upstream and downstream valleys are denoted as $\mathcal{V}_u$ and $\mathcal{V}_d$, respectively.

Pooling configurations

When a valley is separated from the plain by a narrower valley, the pooling configuration referred to in section 3.1, a substantially different behavior is exhibited by the upstream valley once the along-valley wind has developed.

As described in section 3.2, a cold air pool first forms in either valley as a result of the downslope winds and radiative cooling. While a down-valley wind develops next in $\mathcal{V}_d$, starting at the valley exit where the pressure difference between the valley and the plain is the largest, the situation in $\mathcal{V}_u$ is quite different. The cold air pool in $\mathcal{V}_u$ is deeper and colder than in the reference case (Arduini et al., 2016a) because the along-valley wind at the exit of $\mathcal{V}_u$ is first up-valley, as discussed below. A key point is indeed that the cold air pool in $\mathcal{V}_d$ is colder that in $\mathcal{V}_u$, because the former valley is narrower than the latter while the slopes are of similar length and inclination; this effect is all the more pronounced the width ratio between $\mathcal{V}_u$ and $\mathcal{V}_d$ is high. This is attested in Fig. 3a which displays the horizontal pressure difference ΔP between $\mathcal{V}_u$ and $\mathcal{V}_d$ close to the ground: ΔP is negative during an earlier regime, resulting in the up-valley wind at the $\mathcal{V}_u$ exit; it reverses next implying that the along-valley wind becomes down-valley, the air being drained by the down-valley wind which has developed earlier in $\mathcal{V}_d$. Note that ΔP is much smaller than in the counterpart reference cases, implying that the down-valley wind is weaker than in these cases. Figure 3b shows that the down-valley wind is indeed twice smaller close to the ground than in the reference cases at the end of simulations. It is also noticeable that the along-valley wind displays oscillations, well accounted for by McNider (1982) in a simple model combining buoyancy and radiative effects. A final remark is that, in the P2 case, the along-valley wind averaged over the 6 hours of the simulation, namely from late evening to the beginning of the night, has a nearly zero value. Hence, a pollutant emitted in $\mathcal{V}_u$ would hardly travel downstream of its emission location.

The vertical profiles of the along-valley wind are displayed in Fig. 4a (t=150 min) and Fig. 4b (t=360 min). The striking features for the P2 case are the following: at t=150 min, the along-valley wind displays an up-valley jet structure over a height of 200 m or so with a speed of at most $1\,\mathrm{m\,s^{-1}}$; the wind is down-valley above this height up to the plateau level. At the end of the computations (t=360 min), this wind is fully down-valley nearly up to the plateau height with a speed of at most $1\,\mathrm{m\,s^{-1}}$, implying that the return flow (which ensures mass conservation) occurs above the plateau level. In P1, the wind displays an oscillating structure along the vertical, with a higher jet maximum of about $1\,\mathrm{m\,s^{-1}}$. The temporal behavior of the resulting mass flux across a vertical plane at the $\mathcal{V}_u$ exit extending up to the plateau height is displayed in Fig. 4c; this mass flux is normalized by the mass flux for the counterpart reference case. For P2, this non dimensional mass flux is negative during 150 min or so, as expected, but continuously increases during the computation to reach 80% of the reference case mass flux. This result is accounted by the absence of the return flow below the plateau level.

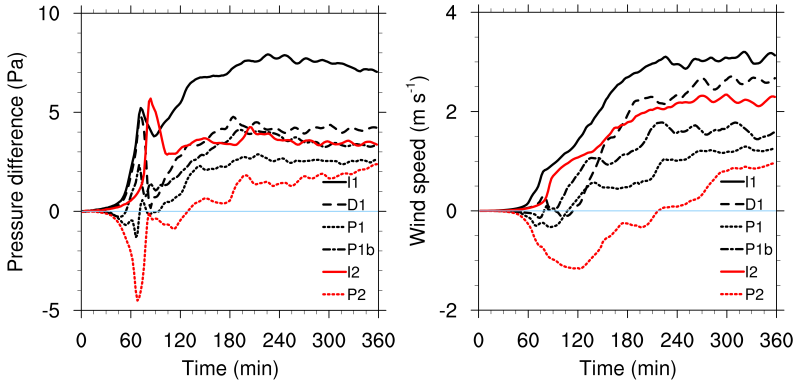

Figure 3: (a) Horizontal pressure gradient between $\mathcal{V}_u$ and $\mathcal{V}_d$, computed along the valley axis at $y = 3$ km for $\mathcal{V}_u$ and $y = 13$ km for $\mathcal{V}_d$, at $z = 25$ m a.g.l., horizontally averaged in the range $180 < x < 180$ m, for the I1 (black solid line), D1 (black dashed line), P1 (black dotted line), I2 (red solid line) and P2 (red dotted line) cases. (b) Time series of the down-valley wind speed at z = 25 m a.g.l., averaged in the range $180 < x < 180$ and $11 < y < 13$ km (i.e. $\mathcal{V}_u$ exit) for the same four cases.

Draining configuration

Let us summarize the main impact of a wider downstream valley on the upstream valley, from Fig. 3 et 4 (D1 case). The potential temperature profile in $\mathcal{V}_u$ is very close to that of I1 at all times but this temperature is colder that in $\mathcal{V}_d$, thereby triggering a down-valley wind. The temperature difference between these two valleys is still smaller than between the upstream valley and the plain (I1 case), implying that the down-valley wind is also weaker than in I1. The return flow develops only from the upper part of the valley implying that, eventually, the mass flux in D1 is 10 % higher than that in I1.

4 Data analysis of the field campaign in the Passy valley

The concentration in PM_{10} recorded at a ground station in the Passy valley during the winter of 2014-2015 is displayed in Fig. 5. The concentration is systematically higher in Passy than in Marnaz and especially Sallanches during persistent inversions, the longest episodes occuring at the beginning of January and in mid-February, during an anticyclonic regime. The purpose of the Passy-2015 field campaign, and counterpart scientific project, was to understand the origin of this behavior from a fluid mechanics point of view.

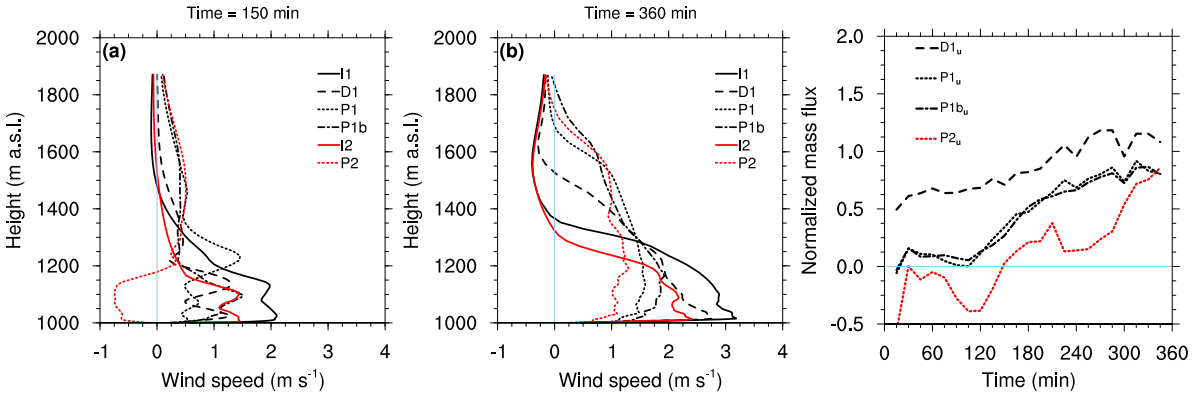

Figure 4: (a) Vertical profiles of the along-valley wind component, horizontally averaged in the range $180 < x < 180$ m and $11 < y < 13$ km (i.e. $\mathcal{V}_u$ exit), at t = 150 min for the I1 (black solid line), D1 (black dashed line), P1 (black dotted line), I2 (red solid line), P2 (red dotted line) cases. (b) Same as (a), but at t = 360 min. (c) Time series of the normalized net along-valley mass fluxes across the surfaces of the $\mathcal{V}_u$ valley centre volumes (defined by $-720 < x < 720$ m and $1000 < z < 1800$ m, at y = 2 km and y = 4 km), for the D1 (black dashed line), P1 (black dotted line), P2 (red dotted line) cases. The mass fluxes are normalized by the mass fluxes in the valleys for the respective reference cases (I1 and I2). The P1b case is not discussed in the paper.

The along-valley wind is displayed in Fig. 6 for January 6th, 2015, along with the concentration recorded at the same location during that day. The measurement site is located in the upstream valley (and not at its exit), using the terminology of the previous analysis, so that the occurrence of an up-valley wind is difficult to assess. Figure 6 shows that the along-valley wind, which is the dominant wind component, oscillates, as already found in the idealized simulations, about a weak negative value. Periods of oscillations of about 30 min and 90 min are found from a spectral analysis. The along-valley wind speed is at most 2 m s^{-1}, which is reached around noon when the wind becomes mostly (because of the oscillations) up-valley for a few hours. Computation of the pdf of the along-valley wind shows that the wind is nearly as often up-valley than down-valley during the day.

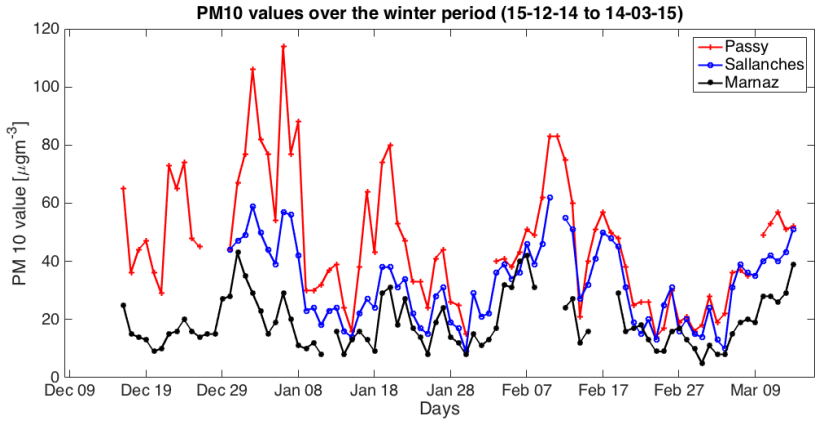

Figure 5: Concentration of PM_{10} (particulate matter of diameter smaller than 10 microns) recorded in the cities of Marnaz, Passy and Sallanches from 15 December 2014 to 15 March 2015. See Fig. 1b for a location of these cities in the Arve valley. The warning threshold of unit50µg m^{-3} is also displayed with a thin black line.

The vertical structure of the along-valley wind is displayed in Fig. 7 at 11 pm, when the PM_{10} concentration is maximum. The figure reveals that a down-valley wind coming from the Chamonix valley detrains at about 300 m, above the measurement station, the

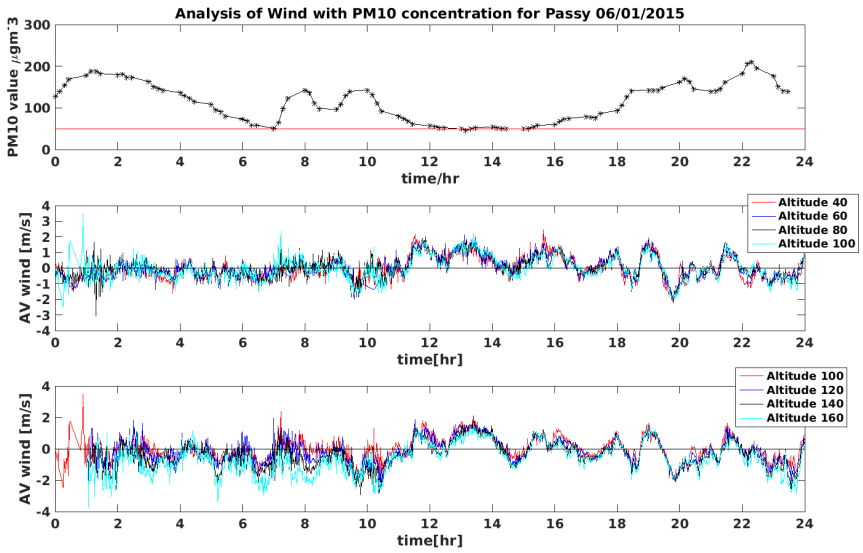

Figure 6: PM_{10} concentration and along-valley wind in Passy for the 6th of January 2015 (top). Time-series of the along-valley wind recorded at the measurement site displayed in Fig. 1b from 40 m to 100 m a.g.l. (middle) and from 100 m to 160 m a.g.l. (bottom). Data recorded by a Lidar WindCube 8 of the air quality agency Atmo Auvergne-Rhône-Alpes.

vertical velocity being very weak close to the ground. The detrainment is very likely due to the presence of a very cold air layer close to the ground, of temperature lower than the air advected by the jet. This would account for turbulence and mixing not occuring close to the ground at 11 pm. From this preliminary analysis, one may suggest a possible explanation for the high concentration recorded in Passy: once emitted, the pollutants travel in a non turbulent stratified fluid back and forth about their emission location, by a distance of at most 1.5 km, and therefore accumulate. This would account for the rise of the concentration to values greater than unit$200 \mu g\, m^{-3}$ during the first part of the night.

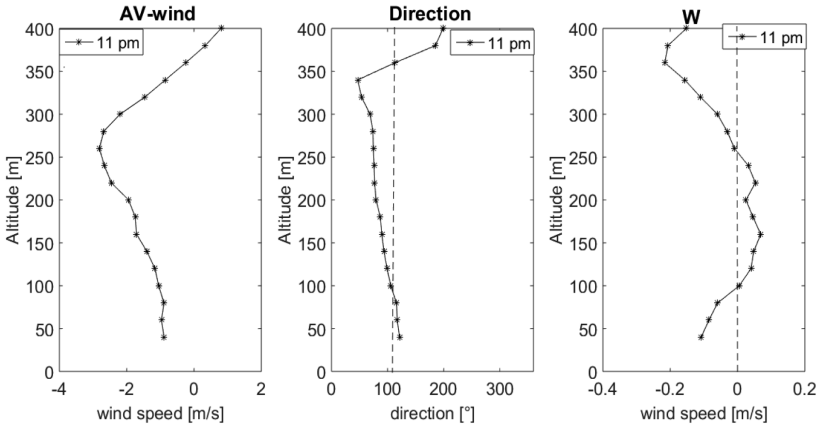

Figure 7: Vertical profiles of long-valley wind speed (left), direction (middle) and vertical velocity (right) at the measurement location displayed in Fig. 1b at 11 pm on January 6th, 2015. The vertical dotted line indicates the along-valley direction at the measurement site. Data recorded by a Lidar WindCube 8 of the air quality agency Atmo Auvergne-Rhône-Alpes and averaged over 10 min.

Figure 6 shows that this argument actually does not apply through the whole night as the PM_{10} concentration decreases during the second part of the night, implying that a ventilation process is at stake. The same analysis carried out at 2 am suggests that

turbulence may occur close to the ground whose origin is currently under investigation.

Acknowledgements

The Passy-2015 field campaign was supported by ADEME through the French national programme LEFE/INSU of CNRS and by METEO-FRANCE. We thank the cities of Passy and Sallanches for their kind support. The field experiment was led by CNRM-GAME while LEGI is the principal investigator of the LEFE/INSU project.

References

Arduini, G., Chemel, C., and Staquet, C. (2016a). Energetics of deep alpine valleys in pooling and draining configurations. *J. Atmos. Science*, submitted.

Arduini, G., Staquet, C., and Chemel, C. (2016b). Interactions between the nighttime valley-wind system and a developing cold-air pool. *Bound. Layer Meteor.*, in press.

Chemel, C., Arduini, G., Staquet, C., Largeron, Y., Legain, D., Tzanos, D., and Paci, A. (2016). Valley heat deficit as a bulk measure of wintertime particulate air pollution in the Arve River Valley. *Atmos. Environ.*, Accepted for publication.

Egger, J. (1990). Observations of thermally developed wind systems in mountainous terrain. 23 (no. 45):57–112.

Lareau, N., Crosman, E., Whiteman, C., Horel, J., Hoch, S., Brown, W., and Horst, T. (2013). The persistent cold-air pool study. *Bulletin of the American Meteorological Society*, 94(1):51–63.

McNider, R. (1982). A Note on Velocity Fluctuations in Drainage Flows. *Journal of Atmospheric Sciences*, 39:1658–1660.

Paci, A., Staquet, C., and and 43 co-authors (2015). The Passy-2015 field experiment: an overview of the campaign and preliminary results. *Proc. of the 33rd International Conference on Alpine Meteorology, Innsbruck, Austria.*

Schmidli, J. and Rotunno, R. (2015). The quasi-steady state of the valley wind system. *Front. Earth Sci.*, Research topic: The atmosphere over mountainous regions.

Silcox, G. D., Kelly, K. E., Crosman, E. T., Whiteman, C. D., and Allen, B. L. (2012). Wintertime PM 2.5 concentrations during persistent, multi-day cold-air pools in a mountain valley. *Atmospheric Environment*, 46:17–24.

Staquet, C., Paci, A., and and 24 co-authors (2015). The Passy project: objectives, underlying scientific questions and preliminary numerical modeling of the Passy Alpine valley. *Proc. of the 33rd International Conference on Alpine Meteorology, Innsbruck, Austria.*

Whiteman, C. (2000). *Mountain meteorology: fundamentals and applications.* Oxford University Press, USA.